



THE UNIVERSITY *of* EDINBURGH

## Edinburgh Research Explorer

### **Correlative 3D Structured Illumination Microscopy and Single-Molecule Localization Microscopy for Imaging Cancer Invasion**

**Citation for published version:**

Pinnington, SJL, Marshall, JF & Wheeler, AP 2018, Correlative 3D Structured Illumination Microscopy and Single-Molecule Localization Microscopy for Imaging Cancer Invasion. in *Correlative 3D Structured Illumination Microscopy and Single-Molecule Localization Microscopy for Imaging Cancer Invasion*. vol. 1764, Methods in molecular biology (Clifton, N.J.), pp. 253-265. [https://doi.org/10.1007/978-1-4939-7759-8\\_15](https://doi.org/10.1007/978-1-4939-7759-8_15)

**Digital Object Identifier (DOI):**

[10.1007/978-1-4939-7759-8\\_15](https://doi.org/10.1007/978-1-4939-7759-8_15)

**Link:**

[Link to publication record in Edinburgh Research Explorer](#)

**Published In:**

Correlative 3D Structured Illumination Microscopy and Single-Molecule Localization Microscopy for Imaging Cancer Invasion

**General rights**

Copyright for the publications made accessible via the Edinburgh Research Explorer is retained by the author(s) and / or other copyright owners and it is a condition of accessing these publications that users recognise and abide by the legal requirements associated with these rights.

**Take down policy**

The University of Edinburgh has made every reasonable effort to ensure that Edinburgh Research Explorer content complies with UK legislation. If you believe that the public display of this file breaches copyright please contact [openaccess@ed.ac.uk](mailto:openaccess@ed.ac.uk) providing details, and we will remove access to the work immediately and investigate your claim.





# Chapter 15

## Correlative 3D Structured Illumination Microscopy and Single-Molecule Localization Microscopy for Imaging Cancer Invasion

Shannon J. L. Pinnington, John F. Marshall, and Ann P. Wheeler

### Abstract

Super-resolution microscopy methods enable resolution of biological molecules in their cellular or tissue context at the nanoscale. Different methods have their strengths and weaknesses. Here we present a method that enables correlative confocal, structured illumination microscopy (SIM) and single-molecule localization microscopy (SMLM) imaging of structures involved in formation of invadopodia on the same sample. This enables up to four colors to be visualized in three dimensions at a resolution of between 120 and 10 nm for SIM and SMLM, respectively.

**Key words** Invasion, Microscopy, Super-resolution, Cells

---

### 1 Introduction

Super-resolution imaging enables an improvement in resolution of the visualization of biological structures in their cellular or tissue context between twice and 20 times [1]. Unfortunately not all methods are created equally, with some methods such as SIM or Airyscan imaging enabling a massive improvement in 3D imaging or visualization of multiple fluorescent labels, but a two-fold resolution improvement. Others such as SMLM methods allow an incredible 20-fold improvement in imaging [2–5] but make it challenging to visualize more than one fluorescent label [6] (Fig. 1). Generally sample preparation methods have meant that a decision has to be made about which super-resolution imaging method will be used for a given sample. This can be disadvantageous where a resolution improvement beyond the 250 nm Abbe limit is required for multiple channels and one or two channels require a considerable increase in resolution. Or it may mean that one scientific question can be answered at the expense of another. In experiments using systems which can be

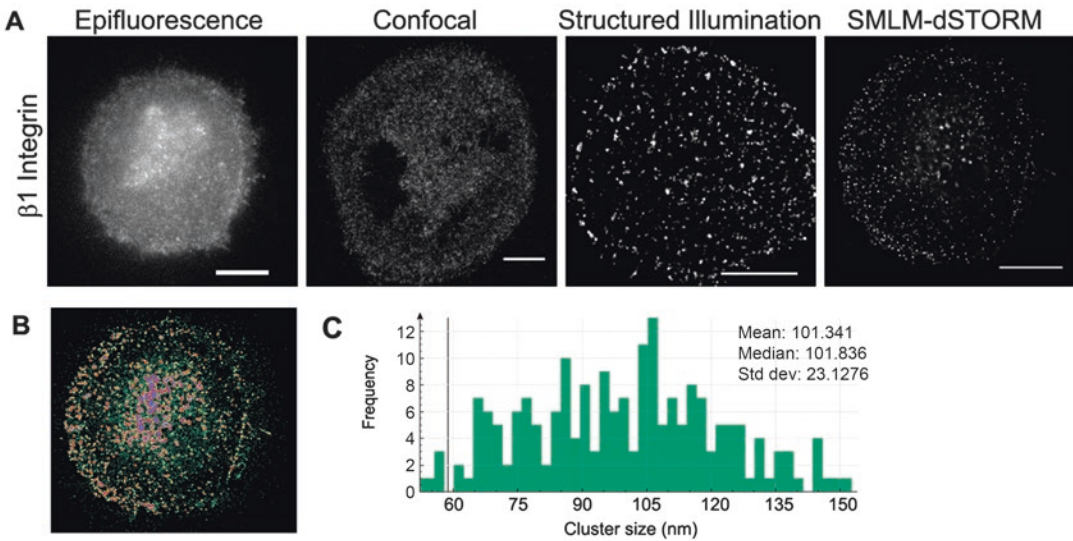


**Fig. 1** Resolution improvement using super-resolution approaches. (a) VB6 oral squamous carcinoma cells stained using mouse anti- $\beta 6$  integrin antibodies and Alexa Fluor 647-labeled FAb2 fragment donkey anti-mouse secondary antibodies as visualized by epifluorescence microscope, confocal microscopy, structured illumination microscopy, and dSTORM single-molecule localization microscopy. Bar = 10  $\mu\text{m}$ . In all cases, images were acquired on a Nikon Ti2 microscope using a 100 $\times$  1.49NA objective. (b) Image showing cluster analysis of dSTORM data using SR-Tesseler. (c) Histograms showing cluster sizes of  $\beta 6$  integrins using the DB scan algorithm in the SR-Tesseler package

more challenging to handle, such as primary cells, organotypic cells, ES cells, and rare tissue samples, this may be less than ideal [7, 8]. Integrins are particularly challenging to image using conventional microscopy as they form small complexes that are spatially close to one another. In conventional microscopy, which is diffraction limited, the blur generated by image diffraction makes these complexes appear to be uniform staining (Fig. 1), although biochemical assays and electron microscopy analyses show this not to be the case [9]. Here we present a method for visualization of up to four structures involved in the process of invasion in transformed cell lines at twice diffraction limited resolution, with an option to allow one of these structures to be visualized to approximately 10 nm resolution with SMLM approaches, using the same sample.

Invadopodia are very small organelles (>2  $\mu\text{m}$ ) which are known to be involved in degradation of the extracellular matrix and have been indicated to play a key role in metastatic spread. They are known to contain metalloproteases, such as MT-MMP1 and MMP9, and can degrade the extracellular matrix (ECM) at focal points (Fig. 2a). The colocalization of the focal degradation and F-actin foci are known as invadopodia [10, 11]. Invadopodia are highly dynamic structures and turn over in minutes [12]. This means at a fixed time point, there will be active invadopodia, indi-

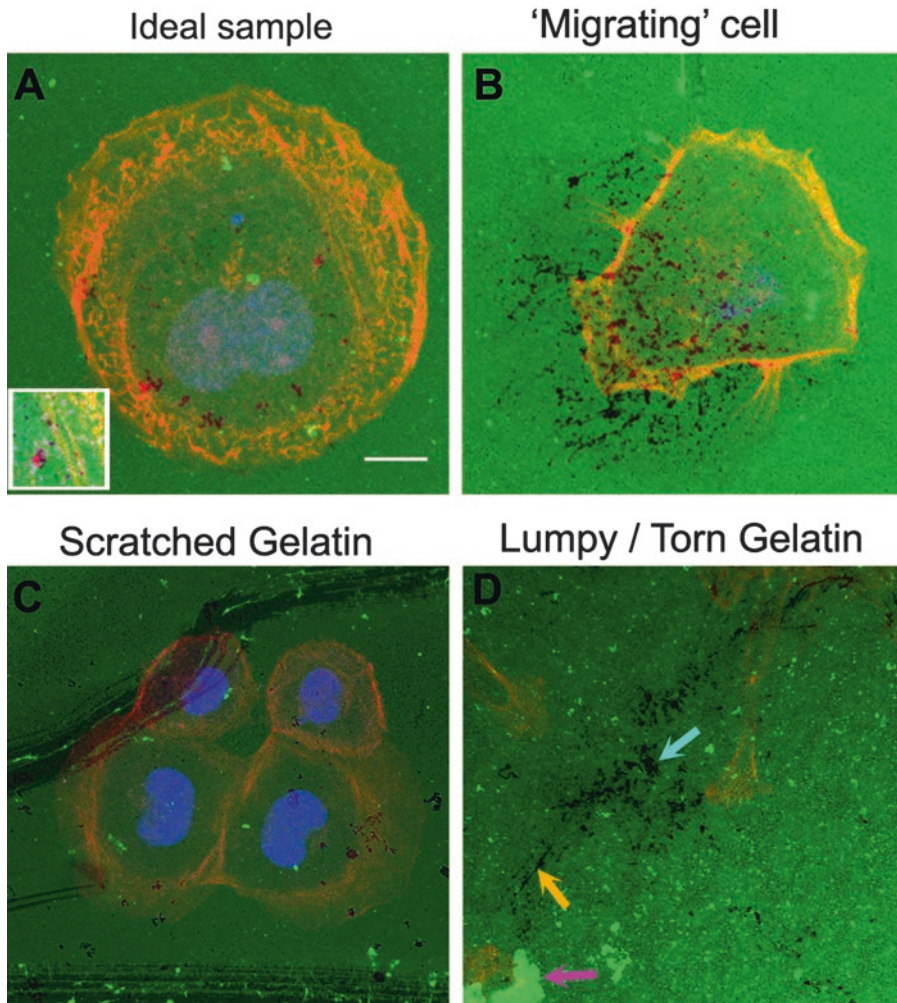


**Fig. 2** Visualization of invadopodia using the gelatin degradation assay. **(a)** A VB6 oral squamous carcinoma cell degrading the gelatin extracellular matrix. Gelatin is shown in green, F-actin in red, and nuclei in blue. Punctate holes in the gelatin indicate invadopodia formation and colocalization of a dot of F-actin and indicate an active invadopodia. **(b)** A cell with a migratory morphology indicates invadopodia has formed and completely turned over. As can be seen, there are around 100 foci which are either under or immediately adjacent to the cell which suggests this cell has recently formed them. For quantification purposes, these invadopodia can be treated as belonging to the cell. **(c)** Scratched gelatin. This occurs when the substrates are mishandled during either cell seeding or fixation. Pipette or forceps mishandling can scratch the fragile gelatin surfaces leading to detachment of the substrate. **(d)** Over-degradation and shearing of gelatin. Here MBA-MB-231 breast carcinoma cells have completely degraded some of the matrix leading to formation of a very large hole—indicated by a cyan arrow. The invadopodia have coalesced into one larger hole, which would, in theory, allow the cell to move through the ECM. These structures can't be quantified as it isn't clear how many invadopodia were present. Shearing of the ECM—long thin lines indicated by an orange arrow—shows where the cell traction forces have stripped the gelatin off the glass coverslip. Either a thicker gelatin layer or a shorter incubation time of cells can reduce this problem

cated by a focus of F-actin colocalized with a hole in the ECM, and invadopodia which have turned over where only a hole in the ECM is present (Fig. 2a). Because of the small size of invadopodia detailed study of which proteins are localized in invadopodia, whether there are phases of protein recruitment to invadopodia, and dynamics, can be challenging. This is mostly because such studies are impeded by the diffraction limit of conventional light microscopes to 200 nm [13]. Using super-resolution, more information can be obtained. However, invadopodia are 3D structures and comprise of several elements—the focal degradation of ECM, localization of F-actin, and recruitment of other proteins such as integrins, which form small complexes.

SMLM imaging of all three of these epitopes over a 6  $\mu\text{m}$  axial range with current equipment is impossible; however, using SIM this is possible, albeit that resolution will be limited to 120 nm. Choice of refraction index-matched coverslips and mounting medium containing anti-fade is important for successful SIM reconstruction. A major mismatch between the setting of the correction collar on the objective lens, the coverslip thickness, and refractive index of the mounting medium can generate spherical aberration artifacts in the final image [14]. The commercial mounting medium Vectashield can be used for SMLM imaging using the dye Alexa-647 and yields images comparable or superior to those obtained with more complex buffers, especially for 3D imaging [15]. We also find that with slight adjustment of the correction collar on our SIM system, combined with the use of high-precision coverslips, correlative SIM/SMLM/confocal imaging of our samples is enabled. For our invadopodia assay, this allows ECM degradation and the F-actin cytoskeleton to be visualized in 3D to 120 nm resolution (Fig. 3). Integrin clusters, providing they are labeled with Alexa Fluor 647 Fab fragments, can then be visualized using 2D STORM SMLM imaging to 10 nm resolution (Fig. 1a) and post hoc analysis of cluster size carried out [16] (Fig. 1b). The following method is used in our laboratory and can be adapted for other applications or proteins by adjustment of the antibodies used at the immunofluorescence stage of sample preparation. Readers must note that the protein for which the greatest resolution improvement is required must be labeled by antibodies labeled with Alexa Fluor 647 dye molecules since Alexa Fluor 647 is compatible with SIM and SMLM.

---

## 2 Materials

1. VB6 cells [17] or other cells with invasive phenotype.
2. Keratinocyte growth medium comprising:  $\alpha$ -MEM containing 10% fetal calf serum (Gibco) supplemented with 100 IU $\text{L}^{-1}$  penicillin, 100  $\mu\text{g/L}$  streptomycin and 2.5  $\mu\text{g/L}$  amphotericin.



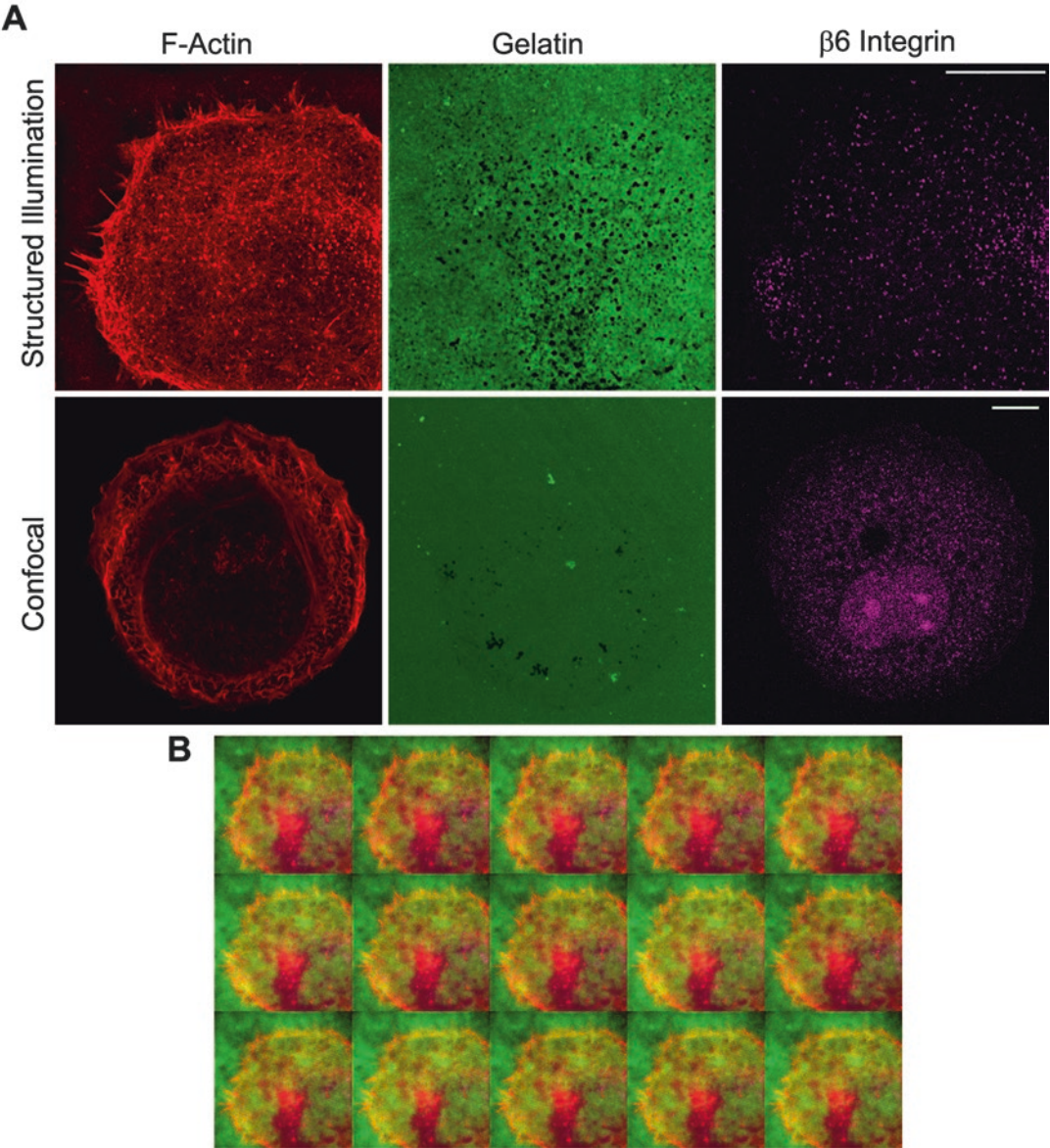


**Fig. 3** (a) A comparison of multicolor structured illumination microscopy and confocal imaging for invadopodia formation. VB6 oral squamous carcinoma cells were seeded onto a gelatin substrate (green) for 6 h and stained for F-actin (red) and β1 integrin (magenta). The montage shows confocal and reconstructed SIM images. Bar = 10 μm. (b) A representative image of the raw SIM dataset used to generate the reconstruction used in (a)

cin B (Gibco),  $1.8 \times 10^{-4}$  M adenine, 5 μg/mL insulin,  $1 \times 10^{-10}$  M cholera toxin, 0.5 μg/mL hydrocortisone, and 10 ng/mL epidermal growth factor (Sigma).

3. High-precision number 1.5 18mm<sup>2</sup> glass coverslips: (ZEISS 474030-9010-000, Marienfeld Cat.No. 0107032, or round 18 mm diameter Cat.No. 0117580).

4. Gelatin from pig skin, Oregon Green® 488 conjugate (Thermo Fisher).
5. 0.5% glutaraldehyde (diluted from a 25% EM grade stock, Sigma).
6. Sodium borohydride NaBH<sub>4</sub> (Sigma-Aldrich).
7. Phosphate buffered saline (Thermo Fisher Scientific).
8. 4% paraformaldehyde (diluted from a 16% EM grade stock VWR resell for Electron Microscopy Sciences).
9. 0.2% Triton x100 (Sigma).
10. 6-well tissue culture plates.
11. Fetal bovine serum (Gibco).
12. Primary antibodies (*see Note 1*): anti-integrin alpha V + beta 6 antibody [10D5] (Abcam); anti-integrin beta 1 antibody [P4C10] (Novus Biologicals).
13. Alexa Fluor 568 Phalloidin (Thermo Fisher Scientific).
14. Alexa Fluor 647 Fab2 anti-mouse (Thermo Fisher Scientific).
15. DAPI (Sigma).
16. Vectashield (Vector Laboratories).
17. Parafilm.
18. Aluminum foil.
19. Nail polish.
20. Fine forceps.
21. Nikon N-SIM microscope equipped with a 100× 1.49NA objective, 405, 488, 561, and 640 nm laser lines Nikon N-STORM/Confocal system equipped with 100× 1.49NA objective and 300 mW 647 nm laser (Nikon Instruments).
22. Fiji ImageJ ([www.fiji.sc](http://www.fiji.sc)) including the following plugins: SIMcheck, ClearVolume.
23. ThunderSTORM software [18] (<https://github.com/zitmen/thunderstorm>).
24. SR-Tesseler [16].

---

### 3 Methods

#### **3.1 Making Gelatin Substrates for Degradation Assay**

1. Put down Parafilm using ethanol to stick flat to tissue culture hood.
2. Defrost gelatin on ice for 6 h prior to experimentation, and spin down gelatin to remove clumps (*see Note 2*).
3. Place 40 µL drops of gelatin onto the Parafilm.
4. Place a coverslip on top of each gelatin drop using the fine forceps.

5. Incubate for 5 min at room temperature in the dark (using foil to cover).
6. Place 40  $\mu\text{L}$  drops of 0.5% PBS glutaraldehyde onto the Parafilm beside the coverslips.
7. Place the gelatin-coated coverslips onto the drops of PBS glutaraldehyde to fix gelatin to the coverslip, using fine forceps to move.
8. Incubate for 15 min at room temperature in the dark.
9. Add >0.5 mL (excess) PBS to a corresponding number of wells of the 6-well plate, and move coverslips into the PBS—gelatin side up.
10. Wash each coverslip twice with PBS.
11. Aspirate off PBS and add >0.5 mL (excess) of PBS  $\text{NaBH}_4$  to each well.
12. Incubate for 3 min in an incubator in the dark (eliminates residual aldehydes).
13. Wash three times with PBS (or until no more bubbles).
14. Aspirate off PBS (*see Note 2*).
15. Add 2 mL cell solution (*see Note 3*) to each gelatin coverslip (*see Subheading 4*).
16. Plates are then incubated for 4–6 h (*see Note 4*) (37 °C, 5%  $\text{CO}_2$ , 100% humidified).

**3.2 Indirect  
Immunofluorescence:  
Fixation,  
Immunolabeling,  
and Mounting**

1. Fix cells in 2 mL 4% paraformaldehyde per coverslip, and leave for 20 min at room temperature.
2. Aspirate off paraformaldehyde and wash four times in PBS. For the fifth wash, leave in PBS for 5 min to remove residual fixative.
3. Aspirate off PBS and add 2 mL 0.2% Triton, and leave for 5 min at room temperature (not in the dark).
4. Aspirate off Triton and wash five times in PBS.
5. Block in 10% FBS for 30 min.
6. Make up solutions of both  $\beta 1$  and  $\beta 6$  primary antibodies (*see Note 4*) and incubate coverslips in a humidified chamber in the dark overnight at 4 °C. 100  $\mu\text{L}$  primary antibody per coverslip is required.
7. Aspirate off primary antibodies and wash 5 $\times$  with PBS.
8. Make up secondary antibody solution Fab AF647 mouse (1:500) (*see Note 1*), phalloidin 568 (1:1000), and DAPI (1:4000), and keep in the dark (wrap microfuge tube in foil) on ice; 100  $\mu\text{L}$  secondary antibody per coverslip is required.
9. Incubate coverslips in secondary antibody in the dark, in a humidified chamber for 1 h at room temperature
10. Aspirate off secondary antibody solution and wash 5 $\times$  in PBS.



11. Mount the stained coverslips in 20  $\mu$ L Vectashield on glass slides, and ensure the coverslips are placed fairly centrally.
12. Affix coverslips to the glass slides using nail polish.
13. Label completed coverslips and leave flat in the fridge to set.
14. Immediately prior to imaging, gently wash the coverslip with double distilled water using a cotton bud wrapped in microscope lens cleaning tissue (*see* **Note 5**).

### **3.3 Super-Resolution Microscopy**

Comparative images using standard, resolution limited imaging methods were acquired using a Nikon Ti Microscope stand and a 100 $\times$  1.49 Apo TIRF objective on the same imaging platform which the dSTORM SMLMs images were acquired. In all cases in the comparative study, the same sample was used for both standard and super-resolution imaging. The epifluorescent image was taken immediately prior to acquisition of the SMLM data of the same cell (Fig. 1a). The confocal images were acquired using a Nikon A1 scan head in Nikon Elements software. The confocal scanhead was attached to the left-hand side port of the Ti microscope and 488, 561, and 647 lasers, similar to the SIM images.

### **3.4 Structured Illumination Microscopy**

1. 3D SIM images are acquired on a N-SIM (Nikon Instruments, UK) using a 100 $\times$  1.49NA lens and refractive index-matched immersion oil (Nikon Instruments). Samples are imaged using a Nikon Plan Apo TIRF objective (NA 1.49, oil immersion) and an Andor DU-897X-5254 camera using 405, 488, 561, and 640 nm laser lines (*see* **Note 5**).
2. To acquire SIM images, set the Z stack collection to range around a center point. Set the center point using the F-actin (568 phalloidin) channel. Set the focal plane corresponding to the bottom of the cell (*see* **Note 6**).
3. A range around the center point of 2  $\mu$ m was set as this allows focused images of the gelatin degradation, actin, and invadopodia-associated proteins to be acquired.
4. For SIM acquisition, the highest laser power and shortest exposure time were selected to minimize photobleaching and speed data acquisition (*see* **Note 7**).
5. Z-step size for Z stacks was set to 0.120  $\mu$ m as required by manufacturer's software. For each focal plane, 15 images (5 phases, 3 angles) were captured with the NIS-Elements software. SIM image processing, reconstruction, and analysis were carried out using the "Stack" option in the N-SIM module of the NIS-Element Advanced Research software. In all SIM image reconstructions, the Wiener and Apodization filter parameters were kept constant. Data were saved in the .nd2 Nikon proprietary format to retain metadata.

6. For a comparator with standard resolution data, datasets were acquired using the N-SIM in wide-field mode. Here the same Z stack was acquired but the grating and phase mask required for SIM acquisition is removed from the microscope light path.
7. Images were checked for artifacts and resolution using the SIMcheck software [19].
8. Data were analyzed for number of invadopodia per cell, integrins, size of invadopodia-mediated degradation using Fiji macros and visualized for presentation in 3D using ClearVolume [20].

### **3.5 Single-Molecule Localization Microscopy**

1. dSTORM images are acquired on an N-STORM system (Nikon Instruments, UK) using a 100× 1.49NA lens and refractive index-matched immersion oil (Nikon Instruments). Images were acquired with the sample illuminated using total internal reflection fluorescence. So only the integrins on the basal surface of the cell could be visualized (*see Note 8*).
2. Samples were imaged using a Nikon Plan Apo TIRF objective (NA 1.49, oil immersion) and an Andor DU-897X-5254 camera, set at EM gain 300 and with conversion settings of 3, using a 640 nm laser lines set at 300 mw power.
3. Images were “back-pumped” using the 647 laser set at 100% until single-molecule photoswitches could be visualized [6]. Datasets of 10,000 images were collected with the camera streamed at 20 Hz. Data was saved as a .tif file and preliminary analysis carried out in the N-STORM software according to manufacturers’ instructions. An estimate of localization precision for the whole dataset was obtained from these analyses (10 nm).
4. Tif stacks were analyzed using ThunderSTORM [18] (*see Note 9*). Images were filtered using the B-Spline wavelet filter with default settings, and molecules were approximately localized using the centroid of connected components, with software default settings. Sub-pixel localizations were assigned using an integrated Gaussian model of the point spread function with a 3 pixel fitting radius and maximum likelihood fitting with an initial sigma of 1.6 assigned for fitting (*see Note 10*).
5. Super-resolution images were visualized using average shifted histograms.
6. Data was drift corrected, filtered with a density filter of 50 nm, and duplicate localizations removed; localizations within a 2 nm radius—likely arising from the same secondary antibody (*see Note 11*)—were merged. Finally localizations with an error of fitting of greater than 100 nm were excluded as they were above the threshold required for clustering.

7. Data tables were exported in .csv format and imported into SR-Tesseler [16] for clustering analysis. Analysis was carried out as described in the paper.
8. Cluster information from DB-Scan and Voronoi segmentation of clusters were exported to Microsoft Excel. Datasets of ten cells per condition were collected for cluster analysis.

---

## 4 Notes

1. Here we visualize integrins  $\alpha\text{v}\beta 6$  and  $\beta 1$  separately. However, any protein with a high affinity and avidity antibody with low background can be used for these assays. It is important to have the protein, which should be visualized in SMLMS labeled with an Alexa Fluor 647 secondary antibody (Figs. 1a and 3).
2. The gelatin coating of coverslips must be carried out with great care. It is essential to either use the coverslips of the size recommended or adjust the amount of gelatin used if a larger coverslip is used so that the coating of the coverslip is completely uniform (Fig. 2a). We recommend aliquotting the gelatin from a stock solution as repeated freeze-thaw cycles degrades the quality of gelling of the gelatin and can cause it to clump. No more than three freeze-thaw cycles for a gelatin aliquot is recommended. Gelatin must be slowly defrosted and centrifuged before use so precipitated gelatin and gelled “clumps” of gelatin are not used (Fig. 2b for an example). While it is challenging to completely avoid clumps, it is very difficult to visualize invadopodia in them, they create an uneven structure for the cells to spread on, and the variation in brightness from the clumps makes batch quantification of images using macros or scripts very difficult. Once the substrate is made, it can be coated with extracellular matrices such as collagen, fibronectin, or laminin or left overnight in an incubator at 37 °C and 5% CO<sub>2</sub> in the dark. Overnight incubation may be desirable as the gelatin degradation assay may take up to 7 h the following day.
3. Cells should be plated in their normal growth medium, and the concentration of cells for the assay should be optimized. Ideally cells should be seeded as a single cell suspension to facilitate visualization of gelatin degradation under the cell. We find concentrations of  $2 \times 10^3$ – $2 \times 10^4$  cells/mL work best, dependent on cell type. Care must be taken when seeding and fixing cells not to accidentally tear the gelatin as this reduces the amount of quantifiable area on the sample considerably; we recommend using very fine forceps for handling and seeding cells using either a Gilson or a 5 mL pipette so the substrate is not accidentally touched (Fig. 2b—scratched substrate).

4. The length of time required for substrate degradation varies dependent on cell type. We find that aggressive cell types such as MBA-MB-231 require 4 h and head and neck squamous carcinoma cell line VB6 requires 6 h. The assay can be refined by fixing the cells at discreet time points after seeding onto gelatin, e.g., 2, 3, 4, 5, and 6 h. If the assay is left too long, the substrate will become too degraded, and it will not be possible to determine where degraded foci corresponding to invadopodia are, or cells may have migrated away from sites of degradation or may have torn the membrane (Fig. 2b—over-degraded gelatin). If insufficient time is allowed for the assay, then no invadopodia will form.
5. The SIM will need to be calibrated with test samples, such as 100 nm TetraSpeck beads (Thermo Fisher Scientific) suspended in Vectashield to minimize spherical aberrations. On Nikon systems, this is carried out by adjustment of the correction collar on the 100 $\times$  objective lens. On other systems, manufacturers should advise. This calibration should be carried out by experienced microscopists only; the system manager, where available, should be approached for advice here.
6. Where possible a whole cell was imaged, when this wasn't possible due to the large size of the cell, a field of view with as much of the lamellipodia/plasma membrane visible was selected (Fig. 3).
7. SIM imaging can be time-consuming, as 15 images need to be acquired to generate one “reconstructed” super-resolution image that is used for quantification and presentation. To speed this process up, fast acquisition times were selected; we found that 30 cells per experimental condition were the minimum we could acquire to obtain statistical robust results and would recommend collection of as many cells/invadopodia as possible (Fig. 3). We recommend retaining both the “Raw” SIM image comprising of the 2  $\mu$ m Z stack of 15 images and reconstructed SIM image as raw data in the study.
8. To reduce drift in SMLM experiments, the imaging system was stabilized to 25 °C, and the Perfect Focus System on our Nikon Ti microscope—which minimizes axial drift—was used. Other microscope manufacturers also have focus feedback, which reduces axial drift (e.g., Definite Focus, Zeiss). We recommend speaking to the manufacturer for advice here.
9. The camera settings were kept constant during SMLM data acquisition and were entered yielding an intensity count to photon conversion factor of 4.8.
10. The SMLM fitting settings for these data were optimized using the ground truth data included in the ThunderSTORM plugin [16]. Ground truth data is a computer-generated dataset with known x, y, z positing which mimics the biological data, which has unknown positions. To optimize the subpixel

fitting conditions, the ground truth data is analyzed using a set of SMLM analysis parameters as described in the method and the goodness of fit determined. The goodness of fit can be described as the Jaccard index which, for SMLM data, is true-positive fits/false-positive fits + false-negative fits. Perfect fitting conditions give a Jaccard index of 1. Here a Jaccard index of 0.9 was obtained [18].

11. Fab2 antibodies are typically labeled with 3.5 dye molecules per antibody. Each dye molecule will photoswitch stochastically, and it is assumed that neighboring dye molecules do not alter this stochastic behavior in these analyses. Therefore, photoswitches within 2 nm are assumed to arise from different dye molecules on the same antibodies and are binned together for the purpose of localization of an individual protein molecule.

## References

1. Galbraith CG, Galbraith JA (2011) Super-resolution microscopy at a glance. *J Cell Sci* 124(Pt 10):1607–1611. <https://doi.org/10.1242/jcs.080085>. 124/10/1607 [pii]
2. Bates M, Huang B, Dempsey GT, Zhuang X (2007) Multicolor super-resolution imaging with photo-switchable fluorescent probes. *Science* 317(5845):1749–1753. <https://doi.org/10.1126/science.1146598>. 1146598 [pii]
3. Huang B, Wang W, Bates M, Zhuang X (2008) Three-dimensional super-resolution imaging by stochastic optical reconstruction microscopy. *Science* 319(5864):810–813. <https://doi.org/10.1126/science.1153529>. 1153529 [pii]
4. Betzig E, Patterson GH, Sougrat R, Lindwasser OW, Olenych S, Bonifacino JS, Davidson MW, Lippincott-Schwartz J, Hess HF (2006) Imaging intracellular fluorescent proteins at nanometer resolution. *Science* 313(5793):1642–1645. <https://doi.org/10.1126/science.1127344>. 1127344 [pii]
5. Rust MJ, Bates M, Zhuang X (2006) Sub-diffraction-limit imaging by stochastic optical reconstruction microscopy (STORM). *Nat Methods* 3(10):793–795. <https://doi.org/10.1038/nmeth929>. nmeth929 [pii]
6. van de Linde S, Löschberger A, Klein T, Heidebreder M, Wolter S, Heilemann M, Sauer M (2011) Direct stochastic optical reconstruction microscopy with standard fluorescent probes. *Nat Protoc* 6(7):991–1009. <https://doi.org/10.1038/nprot.2011.336>. nprot.2011.336 [pii]
7. Cella Zanacchi F, Lavagnino Z, Perrone Donnorso M, Del Bue A, Furia L, Faretta M, Diaspro A (2011) Live-cell 3D super-resolution imaging in thick biological samples. *Nat Methods* 8(12):1047–1049. <https://doi.org/10.1038/nmeth.1744>
8. Hosny NA, Song M, Connelly JT, Ameer-Beg S, Knight MM, Wheeler AP (2013) Super-resolution imaging strategies for cell biologists using a spinning disk microscope. *PLoS One* 8(10):e74604. <https://doi.org/10.1371/journal.pone.0074604>
9. de Rooij J, Kerstens A, Danuser G, Schwartz MA, Waterman-Storer CM (2005) Integrin-dependent actomyosin contraction regulates epithelial cell scattering. *J Cell Biol* 171(1):153–164. <https://doi.org/10.1083/jcb.200506152>. jcb.200506152 [pii]
10. Leong HS, Robertson AE, Stoletov K, Leith SJ, Chin CA, Chien AE, Hague MN, Ablack A, Carmine-Simmen K, McPherson VA, Postenka CO, Turley EA, Courtneidge SA, Chambers AF, Lewis JD (2014) Invadopodia are required for cancer cell extravasation and are a therapeutic target for metastasis. *Cell Rep* 8(5):1558–1570. <https://doi.org/10.1016/j.celrep.2014.07.050>
11. Weaver AM (2006) Invadopodia: specialized cell structures for cancer invasion. *Clin Exp Metastasis* 23(2):97–105. <https://doi.org/10.1007/s10585-006-9014-1>
12. Destaing O, Block MR, Planus E, Albiges-Rizo C (2011) Invadosome regulation by adhesion signaling. *Curr Opin*



- Cell Biol 23(5):597–606. <https://doi.org/10.1016/j.cebm.2011.04.002>. S0955-0674(11)00050-0 [pii]
13. McCutchen CW (1967) Superresolution in microscopy and the Abbe resolution limit. *J Opt Soc Am* 57(10):1190–1192
  14. Demmerle J, Innocent C, North AJ, Ball G, Müller M, Miron E, Matsuda A, Dobbie IM, Markaki Y, Schermelleh L (2017) Strategic and practical guidelines for successful structured illumination microscopy. *Nat Protoc* 12(5):988–1010. <https://doi.org/10.1038/nprot.2017.019>
  15. Olivier N, Keller D, Rajan VS, Gönczy P, Manley S (2013) Simple buffers for 3D STORM microscopy. *Biomed Opt Express* 4(6):885–899. <https://doi.org/10.1364/BOE.4.000885>
  16. Levet F, Hosy E, Kechkar A, Butler C, Beghin A, Choquet D, Sibarita JB (2015) SR-Tesseler: a method to segment and quantify localization-based super-resolution microscopy data. *Nat Methods* 12(11):1065–1071. <https://doi.org/10.1038/nmeth.3579>
  17. Thomas GJ, Hart IR, Speight PM, Marshall JF (2002) Binding of TGF-beta1 latency-associated peptide (LAP) to alpha(v)beta6 integrin modulates behaviour of squamous carcinoma cells. *Br J Cancer* 87(8):859–867. <https://doi.org/10.1038/sj.bjc.6600545>
  18. Ovesný M, Křížek P, Borkovec J, Svindrych Z, Hagen GM (2014) ThunderSTORM: a comprehensive ImageJ plug-in for PALM and STORM data analysis and super-resolution imaging. *Bioinformatics* 30(16):2389–2390. <https://doi.org/10.1093/bioinformatics/btu202>
  19. Ball G, Demmerle J, Kaufmann R, Davis I, Dobbie IM, Schermelleh L (2015) SIMcheck: a toolbox for successful super-resolution structured illumination microscopy. *Sci Rep* 5:15915. <https://doi.org/10.1038/srep15915>
  20. Royer LA, Weigert M, Günther U, Maghelli N, Jug F, Sbalzarini IF, Myers EW (2015) ClearVolume: open-source live 3D visualization for light-sheet microscopy. *Nat Methods* 12(6):480–481. <https://doi.org/10.1038/nmeth.3372>